Science

AAAS

Supplementary Materials for

An intrinsic S/G2 checkpoint enforced by ATR

Joshua C. Saldivar[1], Stephan Hamperl[1], Michael J. Bocek[1], Mingyu Chung[1], Thomas E. Bass[2], Fernanda Cisneros-Soberanis[3,4], Kumiko Samejima[3], Linfeng Xie[5], James R. Paulson[5], William C. Earnshaw[3], David Cortez[2], Tobias Meyer[1] and Karlene A. Cimprich[1]*

Correspondence to: cimprich@stanford.edu

This PDF file includes:

Materials and Methods

Cell culture

      Human hTERT RPE-1 cells (ATCC CRL-4000) were grown in DMEM/F12 medium (Life Technologies 11320-033) supplemented with 10% fetal bovine serum, 100 U/mL penicillin/streptomycin (Thermo Fisher 15140-122) and 10 μg/mL hygromycin B (P212121 GB-T005-20ML). MCF10A cells were grown in DMEM/F12 (Life Technologies 11320-082, no phenol red) supplemented with 5% horse serum (Life Technologies 16050-122), 100 U/mL penicillin/streptomycin (Thermo Fisher 15140-122), 20 ng/mL EGF (PeproTech AF-100-15), 10 μg/mL insulin (Sigma I-1882100 MG), 0.5 mg/mL hydrocortisone (Sigma H-0888), and 100 ng/mL cholera toxin (Sigma C8052-1 MG). HCT116 cells were cultured in McCoy's 5A medium (ATCC 30-2007) supplemented with 10% fetal bovine serum.

Reagents, Antibodies, and siRNAS

      We used small-molecule compounds to inhibit ATR, CHK1, CDK2, CDK1 or WEE1. Inhibitors were dissolved in DMSO (DMSO was used as the mock-treatment). ATRi-1 (AZ20, Selleck Chemicals S7050) was used at 2 μM. ATRi-2 (ATR-45 (*1*)) was used at 2 μM. CHK1i-1 (CHIR-124, Selleck Chemicals S2683) was used at 250 nM. CHK1i-2 (LY2603618, Selleck Chemicals S2626) was used at 1 μM. CDK1i (RO3306) was used at 4.5 μM unless otherwise specified. CDK2i-1 (NU6140) was used at 1 μM unless otherwise specified. CDK2i-2 (KO3861) was used at 5, 10, 15, and 20 μM. WEE1i (MK-1775, Selleck Chemicals S1525) was used at 2 μM. For immunofluorescence microscopy, we used primary antibodies cyclin B1 (Santa Cruz sc-752) diluted 1:500, γH2AX (Cell Signaling Technologies 9718S) diluted 1:500, pFOXM1 T600 (Cell Signaling Technologies 14655S) diluted 1:250, BrdU (BD 347580) diluted 1:100, 53BP1 (BD 612523) diluted 1:500, RPA34 (EMD Millipore NA19L-100UG) diluted 1:1000, H3-pS10 (EMD Millipore 06-579) diluted 1:1000, BLM (Abcam ab2179) diluted 1:500, PCNA (Santa Cruz, SC-56) diluted 1:500), and secondary antibodies goat anti-rabbit IgG Alexa Fluor 647 (Thermo Fisher A21244), goat anti-rabbit IgG Alexa Fluor 488 (Thermo Fisher A11008), goat anti-mouse IgG Alexa Fluor 488 (Thermo Fisher A11001), goat anti-mouse IgG Alexa Fluor 594 (Thermo Fisher A11005), and goat anti-mouse IgG1 (γ1) Alexa Fluor 594 (Thermo Fisher A21125). SMARTpools of ON-TARGETplus siRNAs were used to knockdown FOXM1 (Dharmacon L-009762-00-0005) or B-MYB (Dharmacon L-010444-00-0005). siGL3 (D-001400-01) was used as the control non-targeting siRNA. Individual ON-TARGETplus siRNAs were used to knockdown RAD9A (siRAD9A-1, J-003295-12-0002; and siRAD9A-2, J-003295-11-0002) or ETAA1 (siETAA1-1, J-021193-10-0002; and siETAA1-2, J-021193-11-0002).

Fluorescence microscopy

      Cells were fixed with 4% PFA/PBS for 10 min, permeabilized with 0.25% Triton-X 100 for 15 min, blocked in 1% BSA/PBS for 30 min at RT. For pFOXM1 T600 imaging, cells were fixed with 4% PFA/PBS for 10 min, and permeabilized for 10 min with ice-cold methanol. For pre-extraction of soluble proteins prior to fixing, cells were first permeabilized with ice-cold 0.25% Triton-X 100 for 5 min at 4°C, washed 2x with PBS, and then fixed with 4% PFA. For EdU staining, the Click-iT reaction was carried out following permeabilization using the Click-iT Cell Reaction Buffer kit (Thermo Fisher C10269) and Alexa Fluor 488 Azide (Thermo Fisher A10266) according to the manufacturer's guidelines. For BrdU staining, DNA was denatured

with 2 N HCl for 30 min and neutralized for 10 min with PBS prior to the blocking step. The primary antibodies were diluted in 1% BSA/PBS and incubated overnight at 4°C. Cells were washed 3x with PBS. Secondary antibodies (diluted 1:1000) and DAPI (5 μg/mL) were diluted in 1% BSA and incubated for 1 h at RT. Cells were washed 3x with PBS. For imaging anaphase ultra-fine bridges, cells were grown on coverslips, mounted with Prolong Gold, and images were captured on a Zeiss AxioObserver Z.1, using a 63x PLAN NEOFLUAR NA 1.25 oil immersion objective.

Quantitative image-based cytometry

Cells were grown in 96-well plates (Greiner Bio-One 655090) and imaged on a fully automated ImageXpress Micro (Molecular Devices) at 20x. Analysis of fluorescence intensities was performed using MetaXpress software. Cytoplasmic cyclin B levels were determined by measuring the mean intensity within a ringed mask outside but adjacent to the nucleus. All other intensity measurements were within a nuclear mask generated from DAPI staining. Background levels were determined for each fluorescence marker by assessing histogram plots of the signal intensities in each pixel across several images. The average background value across these images was then subtracted from the mean intensity of the given fluorescent marker in each cell. DNA content was determined by taking the background-subtracted mean nuclear intensity of the DAPI-signal for a given cell and multiplied by the area of the nuclear mask for that cell. Color-coated scatter plots were generated using Tibco Spotfire.

Live imaging and analysis

MCF10A stably expressing EYFP-PCNA and H2B-mTurquoise were seeded into collagen-coated (Advanced Biomatrix 5005-B) 96-well glass plates (In Vitro Scientific P96-1.5H-N) at a density of 15,000 cells per well. Approximately 15 hours later cells were imaged on an atmosphere-controlled ImageXpress Micro XLS every 12 minutes for 8-10 hours. Cells were then treated with DMSO (1:1000) or AZ20 (2 μM). Cells were imaged every 12 minutes for an additional 15 hours in the presence of DMSO or ATRi. In order to validate our automated PCNA puncta calling, we benchmarked S phase cells using a short, 5 minute pulse with EdU (100 μM) in a few untreated wells at the end of each experiment. Following the EdU pulse, cells were fixed and EdU was fluorescently labeled using the Click-IT Cell Reaction Buffer kit (Thermo Fisher C10269) and Alexa Fluor 647 azide (Thermo Fisher A10277). EdU-labelled cells were then re-imaged. Custom scripts were used for automated cell-tracking, PCNA puncta analysis, and EdU benchmarking the start and end of S phase.

FOXM1 phosphorylation profile throughout G2 phase
Live imaging with the EYFP-PCNA biosensor revealed that following an initial rise in pFOXM1 levels at the S/G2 transition, the levels remain steady for nearly 90 min before increasing again as cells approach mitosis (fig. S11). This property allowed us to distinguish early G2 cells based on pFOXM1 levels, and accordingly, we used these levels to gate the early G2 phase cells for the data shown in Figure 2, F and H.

Determination of the EdU incorporation profile of the S/G2 population
We employed a pulse-chase-pulse strategy with EdU and BrdU as a way to define the population of cells that transition into G2 during the EdU pulse (fig. S10A). The assay is based on the principle that cells that transition from S to G2 during the EdU pulse will be BrdU negative, while cells that remain in S phase will be BrdU positive. However, as we increase the gap in between the EdU and BrdU pulse, more of the EdU positive cells will be BrdU negative (they transitioned during the gap). Using this assay we identified the EdU intensity profile of cells that undergo the S/G2 transition during the EdU pulse with 4-8% false-positive rate (fig. S10, B and C). The EdU profile identified in this assay was used to gate the S/G2 cells in Fig. 2, G and H.

mRNA fluorescence in situ hybridization (FISH)
        hTERT RPE-1 cells were grown in 96-well plates (Greiner Bio-One 655090), and pulse-labeled with EdU (30 μM) for 20 minutes either just prior to fixation or prior to thymidine treatment as specified in fig. S9. Cells were fixed with 4% PFA/PBS for 10 min, permeabilized in 0.25% triton-X for 10 min, and EdU was fluorescently labeled using the Click-IT Cell Reaction Buffer kit (Thermo Fisher C10269) and Alexa Fluor 647 azide (Thermo Fisher A10277). PLK1 mRNA FISH was performed using the QuantiGene ViewRNA ISH Cell Assay Kit (QVC0001) and ViewRNA probe (VA1-12113) according to manufacturer's protocol. Images were captured on a Zeiss AxioObserver Z.1, using a 40x Plan-NEOFLUAR NA 0.75 objective.

Cell synchronization
        Asynchronous cells were blocked in S phase with 2 mM thymidine for 24 h. Thymidine was removed and cells were washed 3x with normal growth medium. Cells were released into normal growth medium for 0-8 h. DMSO or ATRi were added 1 h post release from the thymidine block. Cells were then prepped for either RT-qPCR, Western blot, or QIBC analysis.

Western blot
        Cells were lysed on ice with Laemmli Sample buffer supplemented with protease inhibitor cocktail (Sigma P8340), PMSF (1 mM), and beta-mercaptoethanol (5%). Lysates were sonicated, heated to 95°C for 5 minutes, separated by SDS-PAGE, and transferred to PVDF membrane (Millipore IPVH00010). Primary antibodies were rabbit anti-FOXM1 (Bethyl Laboratories A301-533A), rabbit anti-B-MYB (Bethyl Laboratories A301-654A), rabbit anti-Rad9 (Santa Cruz sc-8324), rabbit anti-ETAA1 (Sigma HPA035048), rabbit anti-ETAA1 (2). TOPBP1 (A300-111A-1, Bethyl) CHK1 (sc-8408, G4, Santa Cruz), mouse anti-GAPDH (Abcam ab8245) and mouse anti-alpha-tubulin (Sigma T9026). Secondary antibodies were Goat anti-Rabbit HRP (Molecular Probes G21234) and Goat anti-Mouse HRP (Invitrogen 81-6520).

Chemilluminescence was carried out using the Immobilon HRP substrate (Millipore WBKLS0500), and blots were imaged with a FluorChem HD2 from Alpha Innotech.

siRNA transfection

Cell were seeded at 15,000 cells per well in 96-well plates (Greiner Bio-One 655090) and reverse-transfected with siRNAs at 20 nM mixed with RNAiMAX (Life Technologies 13778030). 16 hours later, growth medium was changed and replaced with normal growth medium. Cells were incubated for a total of 40 h or 48 h post-transfection before the start of experiments.

RNA extraction and RT-qPCR

Total RNA was extracted using Trizol reagent following the manufacturer's protocol. Extracts were digested with RNAse-free DNAse I at 37°C for 30min. Reverse transcription was performed with 1.5 μg total RNA with random hexamer primers and the SuperScript III Reverse Transcriptase Kit. Equal amounts of cDNA were mixed with iTaq SYBR Green Supermix and amplified on a Roche LightCycler 480 Instrument II. mRNA expression levels were measured by the change in comparative threshold cycles using primers to amplify CCNB1, PLK1, CENPF, beta-actin, and GAPDH. mRNA levels were plotted relative to levels in untreated, asynchronous cells. mRNA levels were averaged from two different primer sets normalized to GAPDH and β-Actin mRNA.

Primers for qPCR

CCNB1 left: CGGGAAGTCACTGGAAACAT
CCNB1 right: AAACATGGCAGTGACACCAA

PLK1 left: GACAAGTACGGCCTTGGGTA
PLK1 right: GTGCCGTCACGCTCTATGTA

CENPF left: GTCAGCGACAAAATGCAGAA
CENPF right: ACTCCTGGTCCAGTGTTTGG

beta-actin left: CCTGGCACCCAGCACAAT
beta-actin right: GGGCCGGACTCGTCATACT

GAPDH left: CAAGGCTGTGGGCAAGGT
GAPDH right: GGCCATGCCAGTGAGCTT

Library preparation and RNA-sequencing

mRNA libraries were prepared using the KAPA Stranded mRNA-Seq Kit (KAPA Biosystems KR0960) according to manufacturer's guidelines. Libraries were pooled and sequenced on an Illumina HiSeq 4000 with paired-end 75 bp reads by the Stanford Functional Genomics Facility.

RNA-seq analyses

Reads were aligned to hg19 with tophat, using the Gencode v25 annotations for the sites of transcripts. After alignment, reads were counted over transcripts using HTSeq, and fold-changes and p-values for differences between the transcripts were estimated using the DESeq2 Bioconductor package (GEO accession number GSE116131). Using these fold changes, we focused on the 1767 transcripts in which any sample was significant ($p_{adj} < 0.1$, FDR-corrected Wald Test) in any pairwise comparison. Using the scipy Python library, we clustered these samples using Spectral Biclustering into five groups. We performed GO analysis on each group using the Gene Ontology Consortium's online tool (http://www.geneontology.org/page/go-enrichment-analysis.) We additionally calculated transcription factor ChIP signal around the promoters of the genes in each group. We first obtained FOXM1 ChIP-Seq data from ENCODE (accession number ENCFF000QMR) and B-MYB ChIP-Seq data previously published (GEO dataset GSE27031) (*3*). Using manipulations in Bedtools (*4*), we aggregated the signal around promoters, and plotted the resulting peak shapes using Python, Numpy and Matplotlib. We further defined sets of these 1767 transcripts as being regulated by either B-MYB using the supplemental info of Sadasivam *et al.* (*3*), or by FOXM1 by overlap of the promoter region of the gene in question with peaks called from the same dataset (accession number ENCFF001UMT). We then plotted the fold-changes of genes based on their regulation by these transcription factors, using Seaborn to create kernel-density plots.

Construction of plasmids

     Vector for expression of CDK1as: pT2/SVNeo, a gift from Perry Hackett (Addgene 26553 (*5*)) containing the Sleeping Beauty transposon was modified as follows. pT2/SVNeo was digested with EcoRI and PfoI and then treated with T4DNA polymerase and alkaline phosphatase (Vector). Analogue-sensitive mutant XlCDK1 cDNA (gift of Helfrid Hochegger, University of Sussex) linked to a Zeocin resistance gene via a T2A peptide was digested with NruI and ApaI then treated with T4 DNA polymerase to create the insert. This Insert was ligated with the vector and correct orientation of the insert was confirmed by sequencing.

     Vector for expression of Sleeping Beauty transposase: pCMV(CAT)T7-SB100, a gift from Zsuzsanna Izsvak (Addgene 34879 (*6*)) encodes Sleeping Beauty transposase and was used without modification.

     Vector for inactivation of endogenous CDK1 genes: pX330-U6_Chimeric_BB-cBh-hSpCas9, a gift from Feng Zhang (Addgene 42230 (*7*)) encodes a backbone expressing a guide RNA and Cas9. Double stranded oligonucleotides (5'-CACCGATTTCCCGAATTGCAGTACT-3' and 5'-AAACAGTACTGCAATTCGGGAAATC-3') were inserted into the plasmid following the protocol provided at the Addgene site.

     All restriction enzymes and modifying enzymes were purchased from NEB.

One-shot isolation of RPE1 CDK1as cells

     RPE1 hTERT cells were cultured in DMEM medium supplemented with 10% fetal bovine serum at 37°C with 5% CO_2. To obtain the RPE1 CDK1 analogue-sensitive cell line (RPE1 CDK1as), RPE1 hTERT cells were simultaneously (one-shot) electroporated with 0.5 μg CDK1as expression vector, 0.5 μg Sleeping Beauty transposase expression vector and 0.5 μg endogenous CDK1 gene inactivation vector using a Neon Transfection System (Invitrogen). The electroporation conditions were 2 pulses of 1350 V for 2 ms. Then, the cells were incubated overnight in fresh medium without antibiotics at 37°C. RPE1 CDK1as cells were selected and isolated using 500 μg/mL zeocin and diluted to obtain clones. The resulting clones were

incubated with 5 µM 1NM-PP1 overnight to identify clones that failed to enter mitosis. The presence of the CDK1as mutant in the selected clones was evaluated by Western blot using CDK1 antibody (abcam ab-18). Additionally, functional assays were performed to assess the CDK1as mutant activity by blocking the cells in G2, releasing them and counting the number of mitotic cells. RPE1 CDK1as clones were incubated in 5 µM 1NM-PP1 for 20 h and released into conditioned medium. The cells were fixed with 4% PFA for 10 min and the DNA was stained with DAPI at two time points: 20 h after the blocking and 2 h after the release in conditioned media. RPE1 hTERT cells were used as a control to evaluate the wild type CDK1 activity. A mitotic index was measured to determine the number of mitotic cells.

Synthesis of 1NM-PP1

The ATP analog 4-amino-1-tert-butyl-3-(1'-naphthylmethyl) pyrazolo[3,4-d]pyrimidine (abbreviated 1NM-PP1) was synthesized as described by (8) except that intermediate products 2 and 4, as well as the final product, were isolated by column chromatography before proceeding. The final product, recrystallized from ethyl acetate, was a white solid that gave a single spot when analyzed by thin layer chromatography. Its identity was confirmed by ^{1}H NMR, COSY and high-resolution mass spectrometry. ^{1}H NMR (270 MHz, CDCl$_3$) gave peaks at 1.84 (singlet, 9H), 4.75 (singlet, 2H), 4.85 (broad singlet, 2H), 7.15 (doublet, 1H), 7.38 (triplet, 1H), 7.54 (multiplet, 2H), 7.79-7.92 (multiplet, 2H), 8.22 (doublet, 1H) and 8.24 (singlet, 1H), in close agreement with published data (9). High resolution mass spectrometry gave a mass of 331.181712 for the molecular ion (calculated mass for $C_{20}H_{21}N_5$, 331.179696). Aliquots of the product were dissolved at 25 mM in DMSO just before use.

Generation of TOPBP1-mAID and ETAA1-ΔAAD HCT116 cell lines

ETAA1-Δexon 2 cells were generated using CRISPR/Cas9 as previously described (2). TOPBP1-mAID cells were produced using a system adapted from (10). Briefly, HCT116 parental cells constitutively expressing osTIR1 were generated using CRISPR/Cas9 (Addgene plasmid #72833 and 72834). CRISPR/Cas9 was then used to endogenously tag TOPBP1 by cotransfecting osTIR expressing cells with a guide RNA targeting the last exon of TOPBP1 (GGACTGGATTATCACAAAG) and two homology arm donor vectors containing a mAID cassette with resistance markers to neomycin (Neo) or hygromycin (Hygro). Cells with homozygous editing were selected using 700 µg/ML Neo and 100 µg/mL hygro and validated by western blotting and DNA sequencing. TOPBP1 degradation was induced by addition of 500 µM indole-3-acetic acid (IAA) for two hours.

References

1.   J. D. Charrier *et al.*, Discovery of potent and selective inhibitors of ataxia telangiectasia mutated and Rad3 related (ATR) protein kinase as potential anticancer agents. *J Med Chem* **54**, 2320-2330 (2011).
2.   T. E. Bass *et al.*, ETAA1 acts at stalled replication forks to maintain genome integrity. *Nat Cell Biol* **18**, 1185-1195 (2016).
3.   S. Sadasivam, S. Duan, J. A. DeCaprio, The MuvB complex sequentially recruits B-Myb and FoxM1 to promote mitotic gene expression. *Genes Dev* **26**, 474-489 (2012).

4.   A. R. Quinlan, I. M. Hall, BEDTools: a flexible suite of utilities for comparing genomic features. *Bioinformatics* **26**, 841-842 (2010).
5.   Z. B. Cui, A. M. Geurts, G. Y. Liu, C. D. Kaufman, P. B. Hackett, Structure-function analysis of the inverted terminal repeats of the Sleeping Beauty transposon. *J Mol Biol* **318**, 1221-1235 (2002).
6.   L. Mates *et al.*, Molecular evolution of a novel hyperactive Sleeping Beauty transposase enables robust stable gene transfer in vertebrates. *Nat Genet* **41**, 753-761 (2009).
7.   L. Cong *et al.*, Multiplex Genome Engineering Using CRISPR/Cas Systems. *Science* **339**, 819-823 (2013).
8.   U. Hanefeld, C. W. Rees, A. J. P. White, D. J. Williams, One-pot synthesis of tetrasubstited pyrazoles - Proof of regiochemistry. *J Chem Soc Perk T 1*, 1545-1552 (1996).
9.   A. C. Bishop *et al.*, Generation of monospecific nanomolar tyrosine kinase inhibitors via a chemical genetic approach. *J Am Chem Soc* **121**, 627-631 (1999).
10.   T. Natsume, T. Kiyomitsu, Y. Saga, M. T. Kanemaki, Rapid Protein Depletion in Human Cells by Auxin-Inducible Degron Tagging with Short Homology Donors. *Cell Rep* **15**, 210-218 (2016).
11.   M. Jackman, C. Lindon, E. A. Nigg, J. Pines, Active cyclin B1-Cdk1 first appears on centrosomes in prophase. *Nat Cell Biol* **5**, 143-148 (2003).

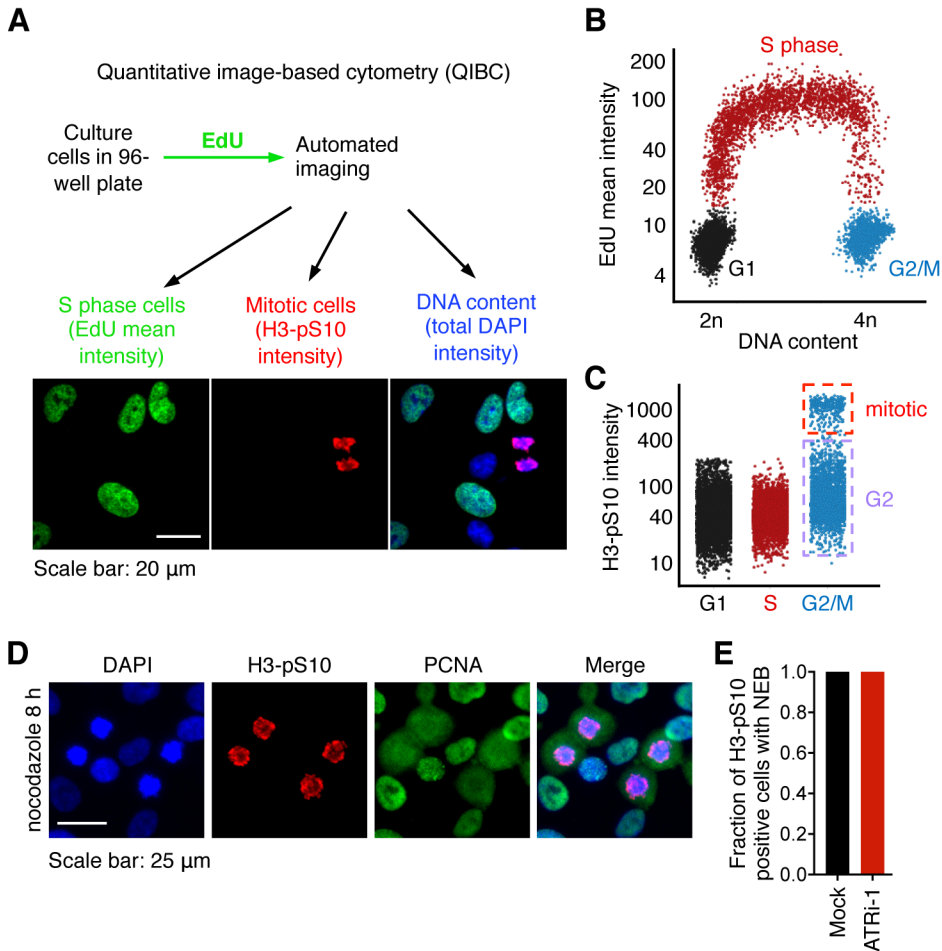**Author Contributions:**

fig. S1

fig. S1. Analysis of cell cycle using quantitative image-based cytometry (QIBC). (**A**) Using a high-content fully automated microscope, thousands of cells are imaged per experimental condition yielding quantitative data on DNA content (total DAPI intensity) and cell cycle markers. The data is plotted similarly to flow cytometry data. To label S phase cells, the cells are pulsed with EdU (10 μM) for 20 min. Immunofluorescence is used to quantitatively image cell cycle markers (e.g. H3-pS10, a mitotic marker) or other signals. Representative images of hTERT RPE-1 cells stained for EdU, H3-pS10, and DAPI. (**B**) Plots of individual cells based on EdU mean intensity and total DAPI intensity. Colored dots indicate the labeled cell cycle phase. (**C**) Plots of H3-pS10 mean intensity in the G1, S, or G2/M populations. Note that the G2/M subpopulation shows a bimodal distribution of the H3-pS10 signal, distinguishing the G2 and mitotic cells. (**D**) Representative images of cells arrested with nocodazole for 8 h. PCNA was used to visualize nuclear envelope breakdown (NEBD). (**E**) Fraction of mitotic cells, as determined by H3-pS10 intensity, exhibiting NEBD. Cells were mock- or ATRi-treated for 8 h.

fig. S2

A

S or G2 to M progression assay

washoff

EdU → nocodazole +/- ATRi (0-10 h) → Image DAPI, EdU, H3-pS10

B
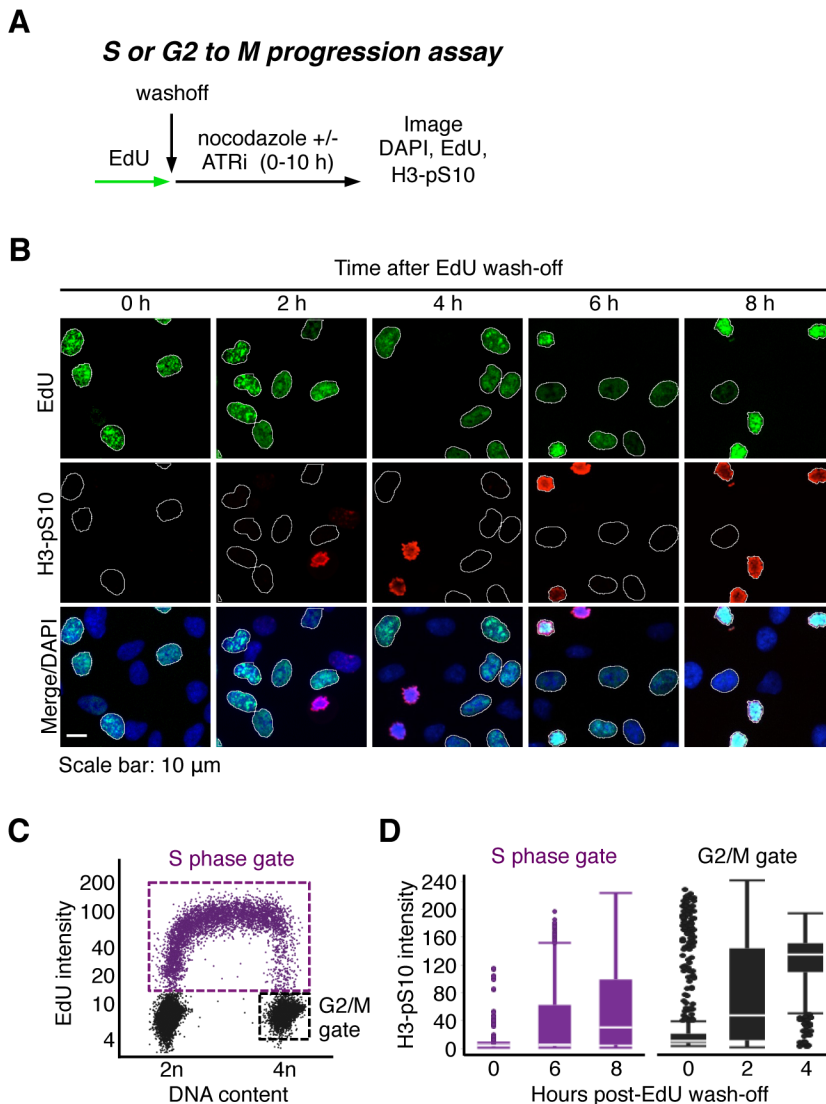

Scale bar: 10 μm

C

D

fig. S2. Assay of S-M or G2-M progression. (A) Experimental design. Cells were pulsed with EdU (10 μM) for 20 min, then washed 2x with PBS, and incubated in the presence of nocodazole (50 ng/mL) for 0-10 h. Inhibitors of ATR were added during the nocodazole treatment. After 0-10 h, cells were fixed and imaged for DAPI, EdU, and phosphorylated histone H3 Ser10 (H3-pS10). **(B)** Representative images of cells at indicated timepoints following EdU wash-off. Dotted lines encircle the EdU-positive cells. **(C)** Scatter plot illustrating the S phase and G2/M gates from a sample experiment at T=0. **(D)** Box and whisker plots of the H3-pS10 signal intensities in the S-phase or G2/M-gated populations at the indicated timepoints following EdU wash-off. Boxes denote the 25th percentile, median, and 75th percentile. Whiskers extend to the upper and lower adjacent values. Dots indicate cells above or below adjacent values.

fig. S3

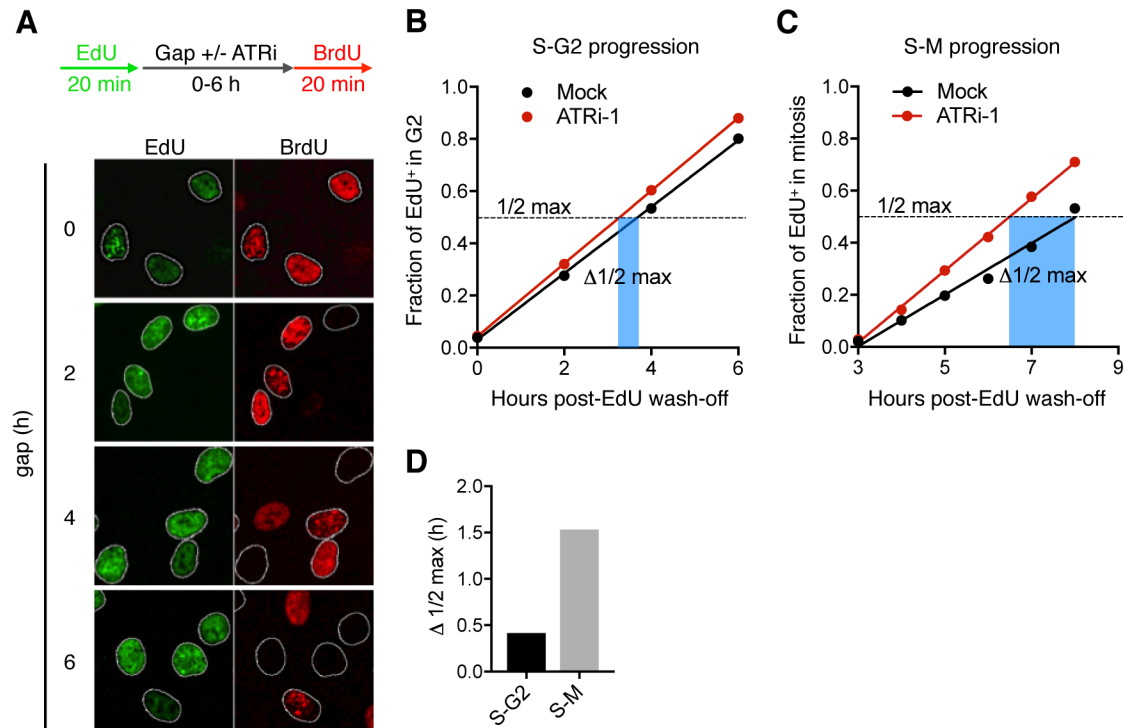

fig. S3. Pulse-chase-pulse assay to measure S-G2 progression. (A) S-G2 progression assay. Cells were pulsed with EdU (10 μM) for 20 min, then washed 2x with PBS, and chased for 0-6 h. During the chase, cells were either mock- or ATRi-treated. Cells were then pulsed with BrdU (50 μM) for 20 min and then fixed and stained for DAPI, EdU, and BrdU imaging. Representative images of cells at indicated timepoints following EdU wash-off. Dotted lines encircle the EdU-positive cells. (B) Fraction of EdU-positive cells that progressed to G2 phase (BrdU-negative) during the chase. Blue-shaded box indicates the change (Δ) in time on the x-axis between the half-max values of the mock and ATRi on the y-axis (1/2 max) (C) S-M progression assay shown in Fig. 1, A and B. Data reshown here for comparison of the Δ ½ max value. Note the difference in S-G2 caused by ATRi is less than the difference of S-M. (D) Charts of the Δ ½ max values between mock and ATRi for S-G2 and S-M rates of progression.

fig. S4

A

Scale bar: 5 μm

B

C

D

E

hours since S phase start:

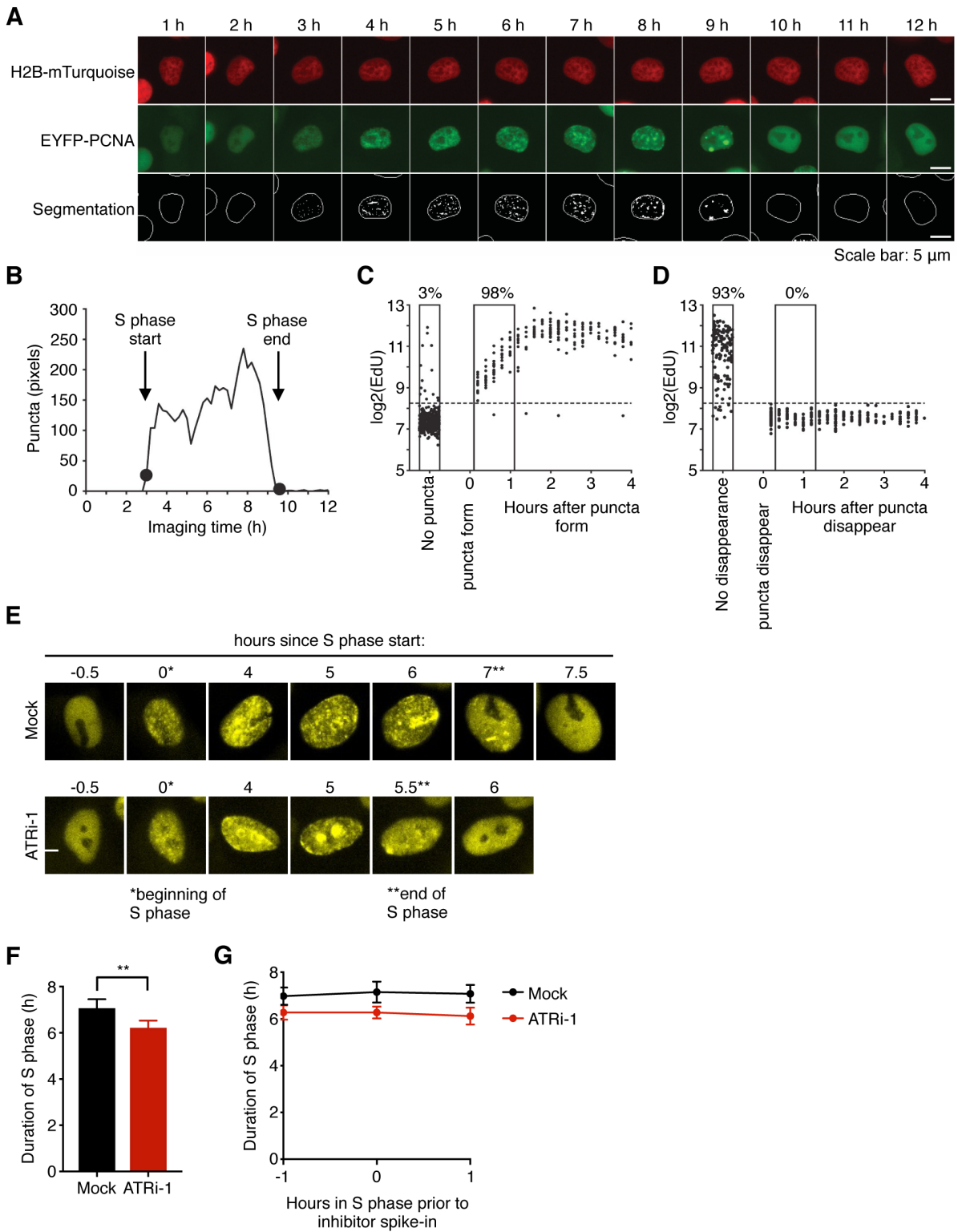*beginning of S phase   **end of S phase

F

G

fig. S4. Live-imaging analysis of S phase duration using the PCNA biosensor. (A) Time-lapse images of an individual MCF10A cell expressing H2B-mTurquoise and EYFP-PCNA.

Segmentation shows EYFP-PCNA puncta. EYFP-PCNA puncta formation marks the start of S phase, and puncta disappearance marks the end of S phase. (**B**) Trace of the time of PCNA puncta formation and disappearance in an individual cell. The black dots mark the start and end of S phase. (**C and D**) EdU-benchmarking to validate PCNA-puncta formation and disappearance as markers of the start and end of S phase. At the end of each live-imaging experiment, cells were pulsed for 5 min with EdU (100 μM) and then fixed. Cells were re-imaged, and the EdU intensity was measured and plotted as a function of time after puncta form or disappear. Percentages indicate the accuracy of calling the S phase start and end times based on puncta formation and disappearance. (**E-G**) Duration of S phase analysis by live-imaging of the EYFP-PCNA biosensor. (E) Representative images of EYFP-PCNA at indicated times relative to the start of S phase. Asterisks denote the start and end of S phase. Cells were imaged for 8 h at 12 min intervals, spiked with the mock or ATRi, then imaged for an additional 15 h. (**F**) Duration of S phase determined from live-imaging of EYFP-PCNA. Error bars represent the SEM of 4 independent experiments. Paired student t-test was used to calculate the p-value. **$p <$ 0.01. (**G**) Duration of S phase as a function of hours in S phase prior to addition of inhibitor.
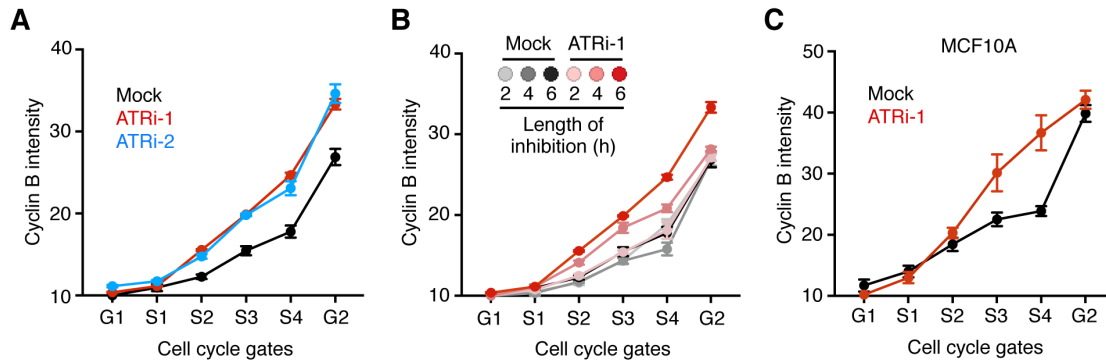
fig. S5

fig. S5. ATR inhibition results in premature accumulation of cyclin B1 in late S phase. (**A**) Mean cyclin B cytoplasmic intensities of gated populations as described in Fig 1F. The mitotic population was excluded. Error bars represent the SEM of cells within each gate. hTERT RPE-1 cells were mock- or ATRi-treated with two different ATR inhibitors for 6 h. (**B**) Mean cyclin B cytoplasmic intensities as described in (A). Cells were mock- or ATRi-treated for 2, 4, or 6 h. (**C**) Mean cyclin B cytoplasmic intensities in MCF10A cells treated as in (A).

fig. S6

A

Seed RPE-1 → Thymidine block 24 h → Wash and release → Inh added 1 h after release → RNA isolation (0-8 after release)

B

C

D

E
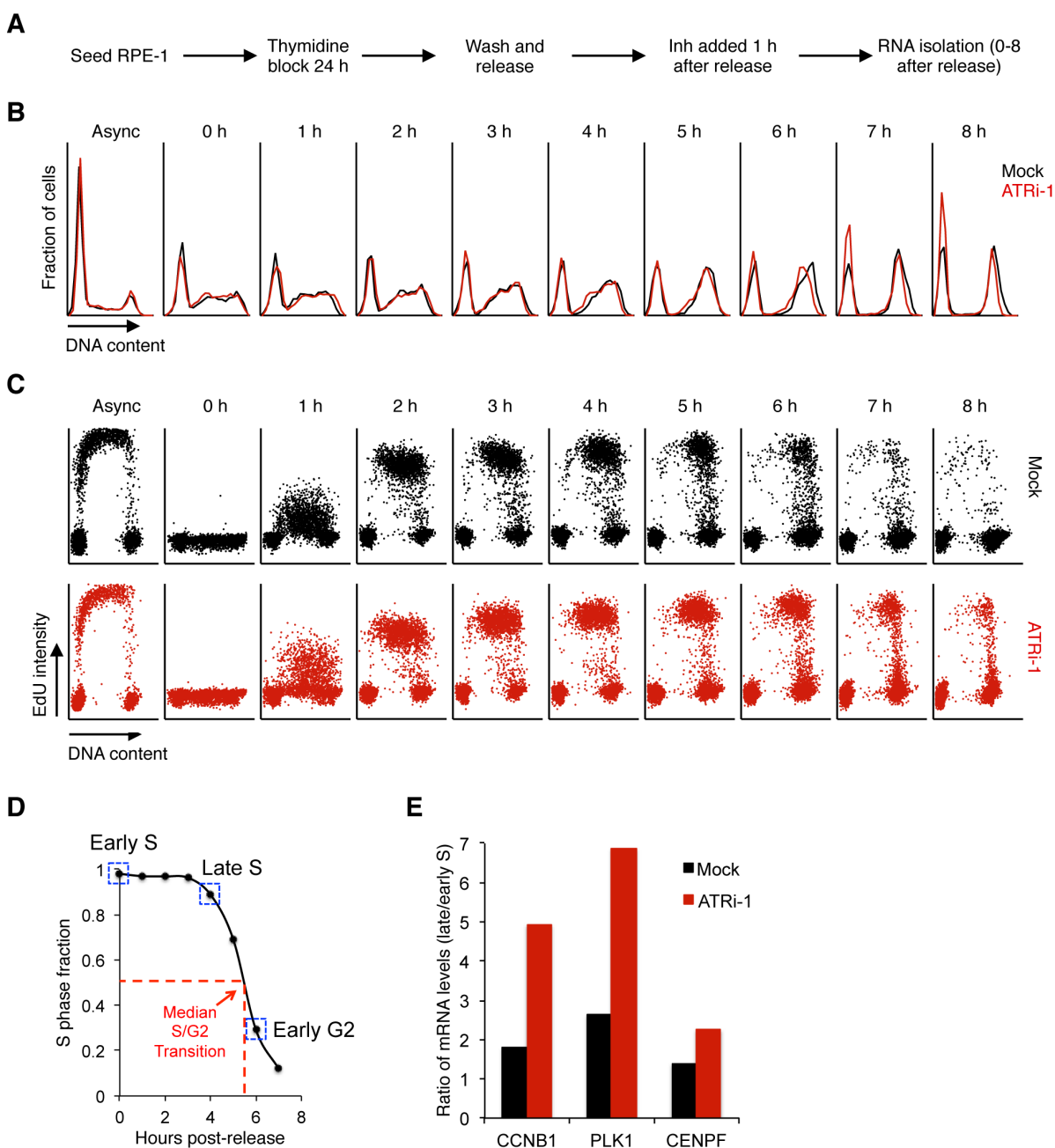
fig. S6. Cell cycle analysis of thymidine synchronized cells. (**A**) S phase synchronization experimental design using thymidine (2 mM) block and release. Cells were mock- or ATRi-treated 1 h following release. RNA was isolated at 0-7 h following release. (**B**) Histograms of DNA content as determined by total DAPI intensity. Cells were synchronized as described in (A). (**C**) QIBC plots of EdU mean intensity versus DNA content for cells synchronized in (A and B). Cells were pulsed with EdU for 20 min prior to fixation. (**D**) Plot of S phase fraction and time post-release. S phase fraction is defined as the fraction of S phase cells that are still in S phase (EdU-positive) at each timepoint following release. The median S/G2 transition is the time at which half of the S phase population has moved into G2. Blue boxes indicate the timepoints

used for the RNA-seq experiment in Fig. 1H. (**E**) RT-qPCR analysis of cyclin B1, PLK1, or CENPF mRNA from cells synchronized as described in (A). Bars show the average ratios of mRNA levels in late/early S phase from 3 independent experiments.
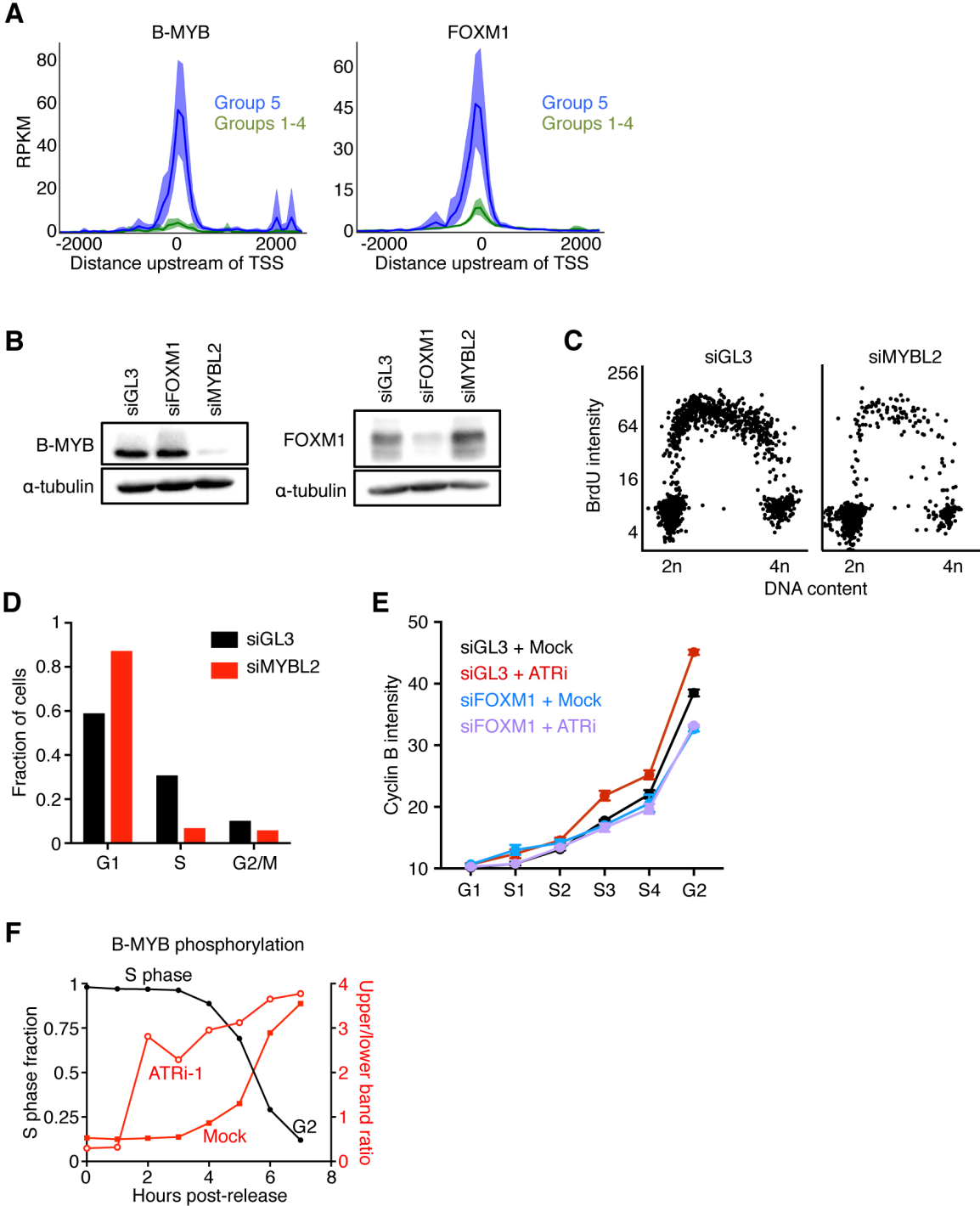
fig. S7

fig. S7. B-MYB and FOXM1 promote expression of group 5 genes. (**A**) Enrichment of B-MYB or FOXM1 at promoters aligned at the transcription start site (TSS) of group 5 genes or groups 1-4 genes using publically available ChIP-seq datasets (see Supplemental Materials for a detailed description). (**B**) Western blots in hTERT RPE-1 cells 40 h after transfection with a control siRNA (siGL3) or siRNAs targeting FOXM1 (siFOXM1) or B-MYB (siMYBL2). (**C**)

17

XY plots of BrdU mean intensity and total DAPI intensity 40 h after transfection with siRNAs. Cells were pulsed with BrdU (25 μM) for 20 min prior to fixation. (**D**) Fraction of cells in the different cell cycle phases based on BrdU and DAPI plots in (C). (**E**) Mean cyclin B cytoplasmic intensity in hTERT RPE-1 cells. Cells were transfected with control siRNA (siGL3) or siRNAs targeting FOXM1 (siFOXM1), and 40 h later, cells were treated and analyzed as described in Fig. 1F. (**F**) The ratios of the upper to lower B-MYB band intensities from Western blots shown in Fig. 2A. Ratios are plotted as red lines on the right y-axis. Black lines are XY line plots of the fraction of S phase synchronized cells and are plotted on the left y-axis. S phase fraction was calculated as described in fig. S6, B-D.
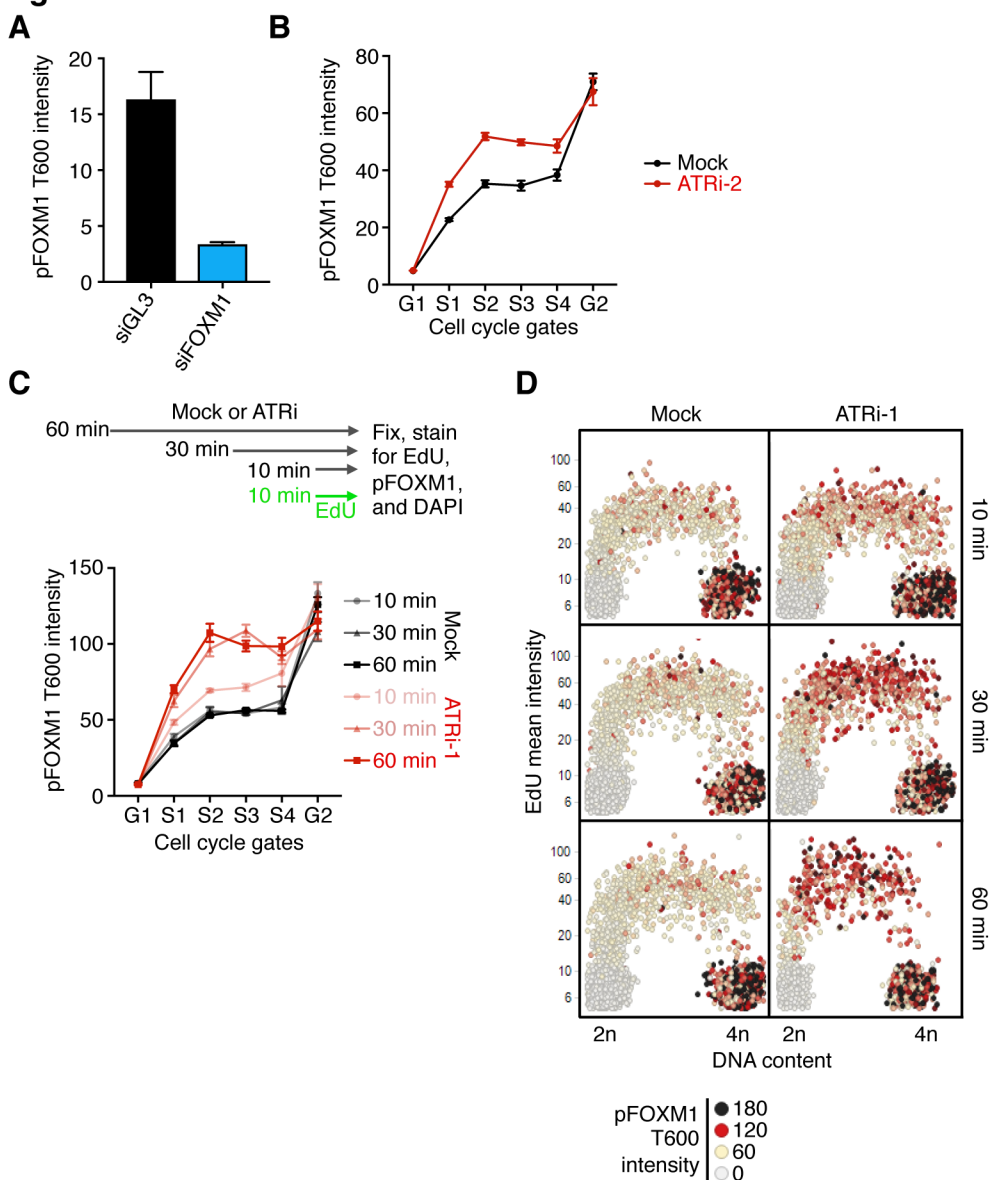
fig. S8. Analysis of FOXM1 phosphorylation at T600 in single cells. (**A**) pFOXM1 T600 intensity 40 h post transfection with siGL3 or siFOXM1 siRNA. Columns and error bars denote the medians and 95% confidence intervals, respectively. (**B**) Median pFOXM1 intensities of gated populations (See Fig. 2D) following ATRi with a second inhibitor (ATR-45, 2 μM). (**C**) Experimental design and median pFOXM1 intensities of populations gated as in Fig 2D. (**D**) QIBC plots of total DAPI intensity vs. EdU mean intensity, and mean pFOXM1 T600 intensity on a color scale.
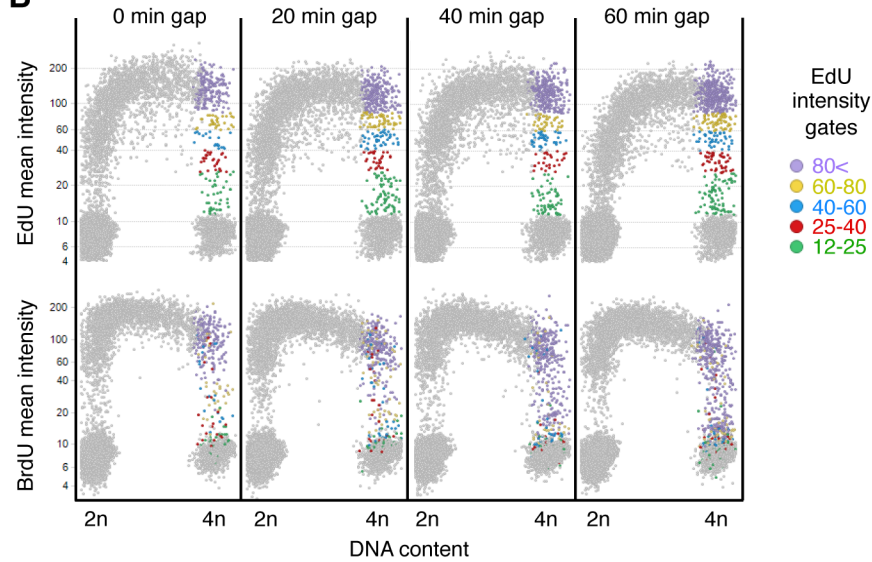
fig. S9
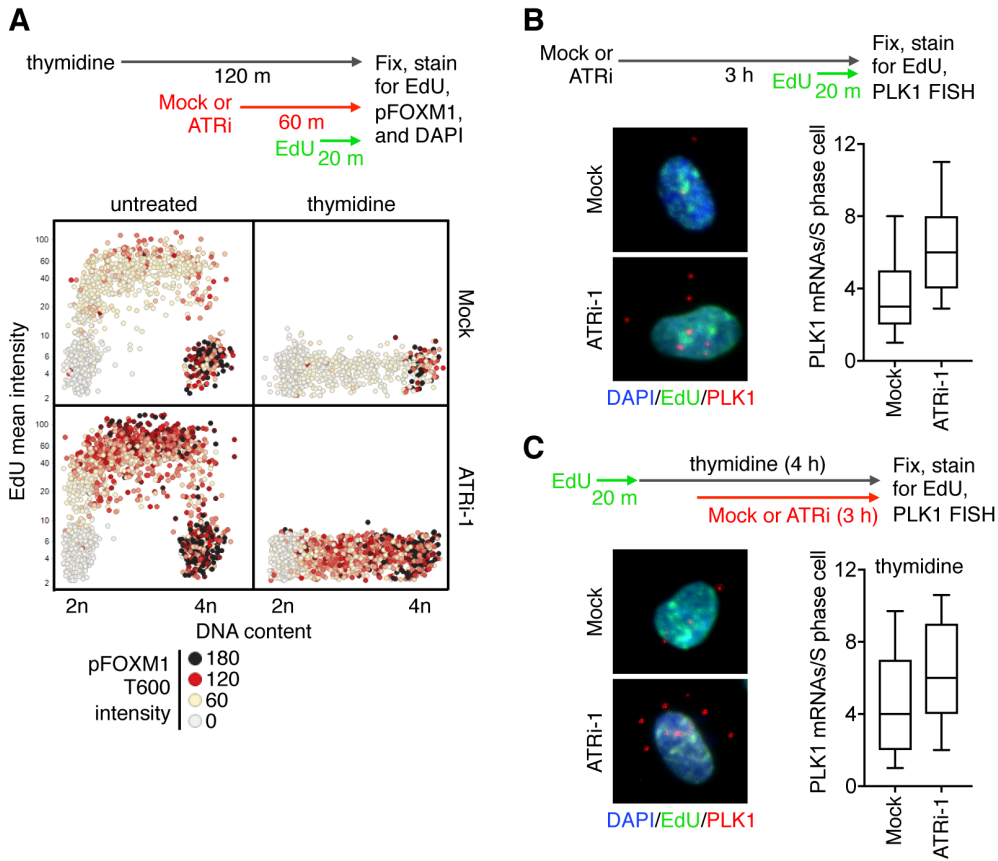
fig. S9. Premature phosphorylation of FOXM1 and expression of PLK1 following ATRi during a thymidine block. (**A**) Experimental design and QIBC plots of total DAPI intensity vs. EdU mean intensity, and mean pFOXM1 T600 intensity on a color scale. (**B and C**) Experimental design, representative images of PLK1 mRNA fluorescence in situ hybridization (FISH), and number of PLK1 mRNAs in mock-treated (B) or thymidine-blocked (C) cells.
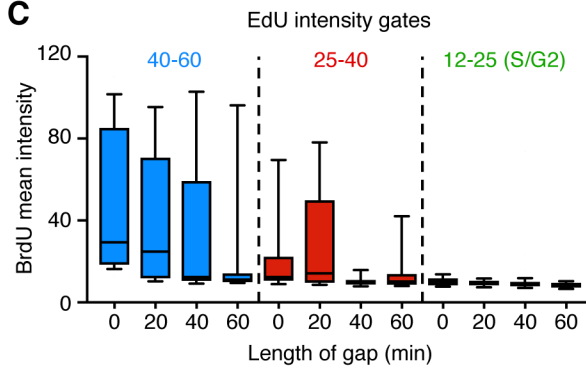
fig. S10

A

EdU — Gap — BrdU — Fix, stain EdU,
20 min — 0-60 min — 20 min — BrdU, DAPI

B

EdU intensity gates

- 80<
- 60-80
- 40-60
- 25-40
- 12-25

C

EdU intensity gates

40-60   25-40   12-25 (S/G2)

Length of gap (min)
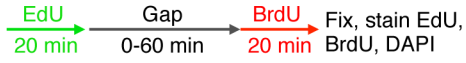
fig. S10. Pulse-chase-pulse assay to identify the S/G2 population. (**A and B**) Experimental design and QIBC plots of total DAPI intensity vs. EdU mean intensity and BrdU mean intensity. Note the late S phase population is colored based on EdU mean intensity. (**C**) Plots of the BrdU mean intensity of the different late S phase populations at each gap length. Color schemes match those from B. The lack of BrdU incorporation in the late S population with EdU intensities between 12-25 indicate these cells transitioned from S to G2 during the EdU pulse.
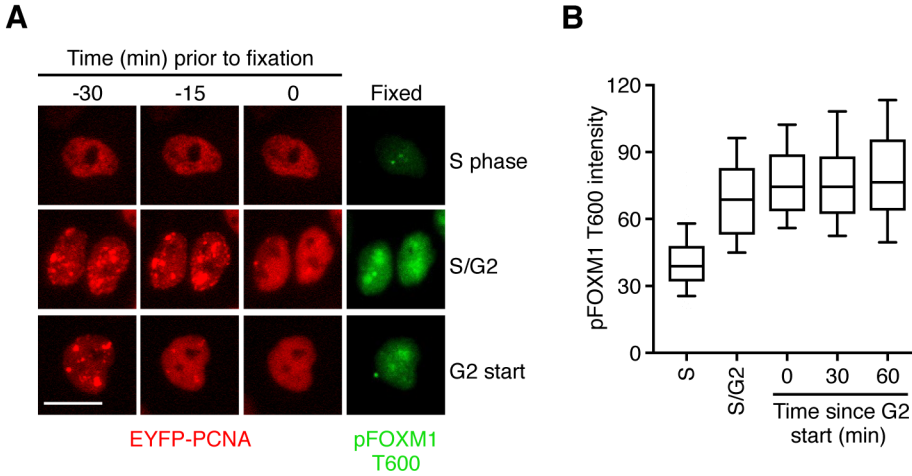
fig. S11

A

Time (min) prior to fixation

-30 -15 0 Fixed

S phase

S/G2

G2 start

EYFP-PCNA   pFOXM1 T600

B

fig. S11. Live imaging of S/G2 transition and pFOXM1 T600 levels. (**A**) Representative time-lapse images of MCF10A cells expressing EYFP-PCNA and immunofluorescence staining of pFOXM1 T600 following fixation. S phase cells, cells at the S/G2 transition, or the start of G2 were identified based on the pattern of PCNA puncta. In the time-lapse images, the PCNA puncta become enlarged and only a few are present as cells near the end of S phase. In the last image prior to puncta disappearance (S/G2 cells) the enlarged puncta become significant smaller and EYFP-PCNA becomes more diffuse in appearance. This progression is clearly seen in the G2 start images above from -30 to -15 minutes prior to fixation and in the S/G2 images above from the -15 to 0 minute prior to fixation. (**B**) pFOXM1 T600 mean intensity of MCF10A cells following live-imaging and fixation.
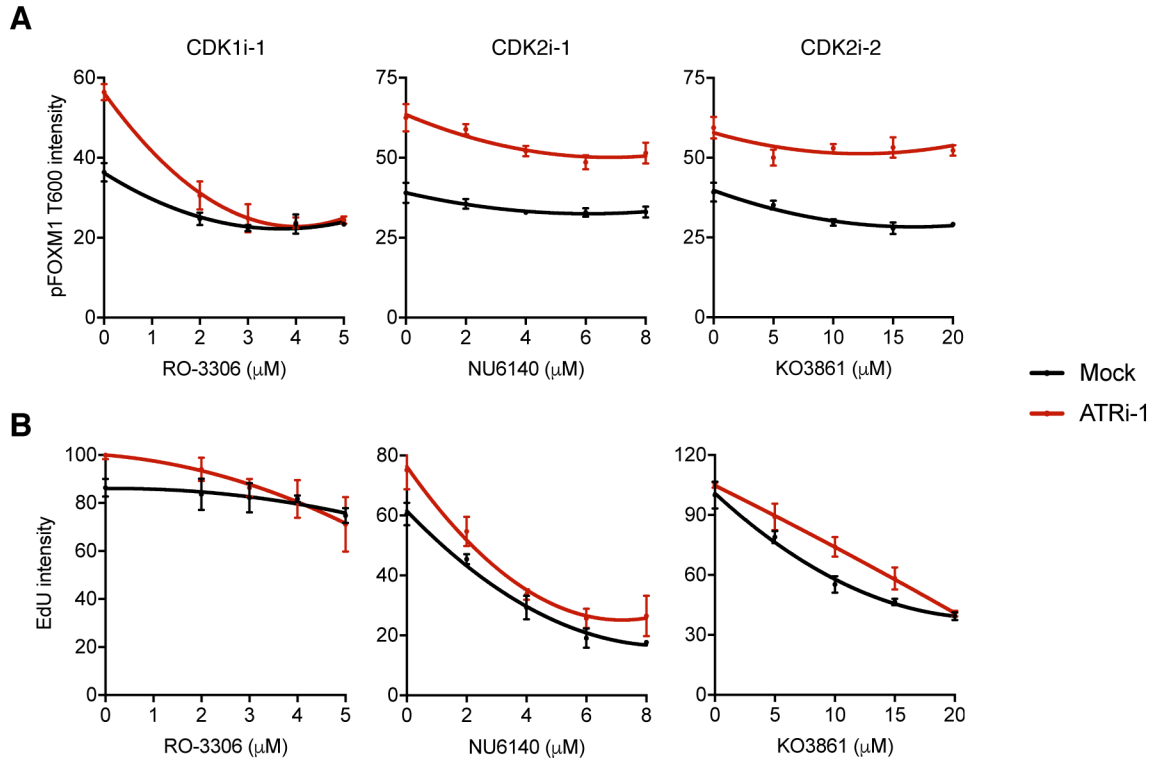
fig. S12

A

B

fig. S12. CDK1 and CDK2 inhibitor dose-response curves. (**A**) pFOXM1 T600 levels in S phase cells as a function of concentration of the three different CDK inhibitors. The CDK and ATR inhibitors were added for 1 h and S-phase cells were labeled with EdU for the final 20 minutes. (**B**) EdU mean intensity in S phase cells as a function of concentration of the three different CDK inhibitors.

A

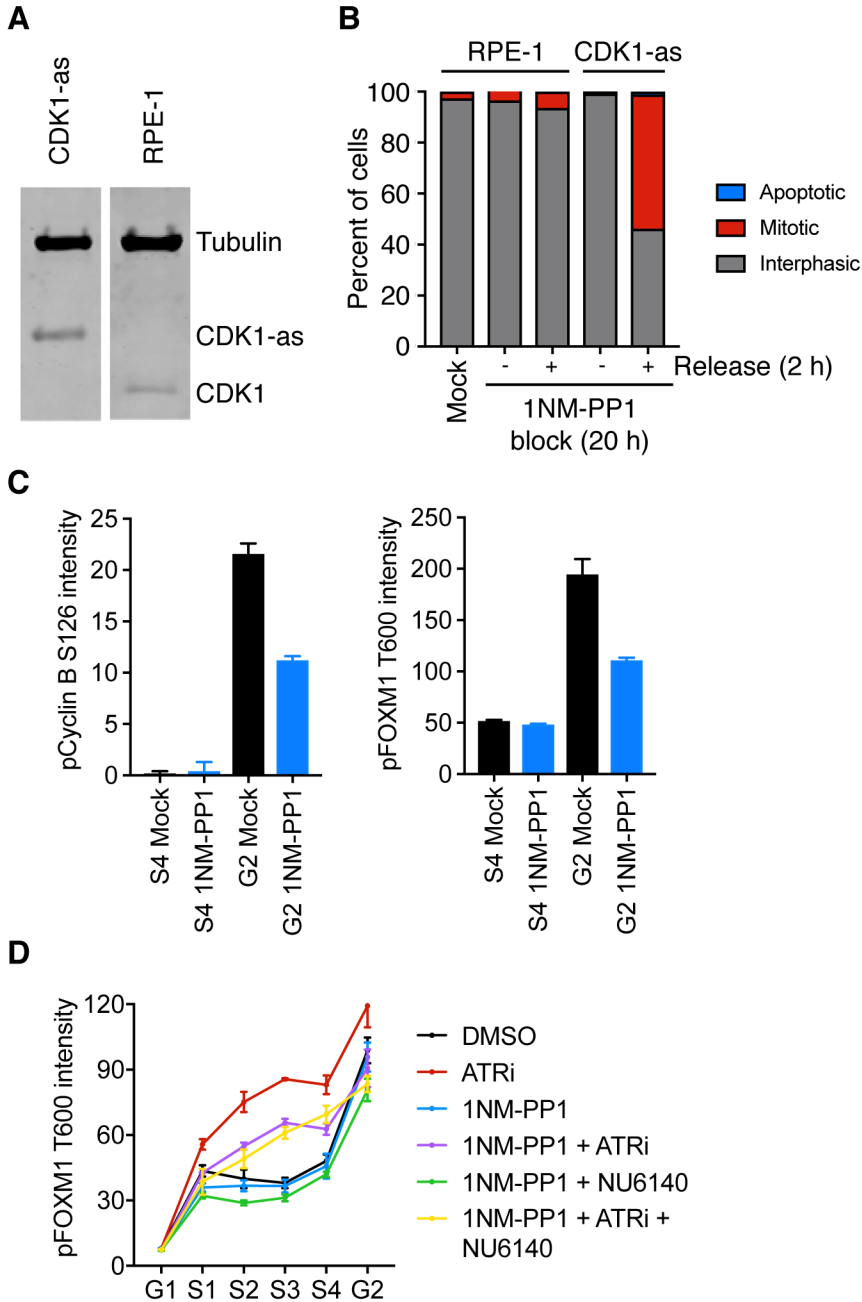
B

C

D

fig. S13. Characterization of a CDK1-as RPE-1 cell line and validation of CDK1-mediated FOXM1 phosphorylation. (**A**) Western blot analysis of select clones confirming the presence of the CDK1-as allele in RPE-1 cells. (**B**) Cell cycle analysis following a G2 block with the CDK1-as inhibitor 1NM-PP1 (5 μM) for 20 h and a 2 h release into conditioned medium. (**C**) The mean and SEM pCyclin B S126 intensity and pFOXM1 T600 intensity of late S (S4) and G2 phase cells either mock-treated or 1NM-PP1-treated for 1 h. pCyclin B S126 is a CDK1-cyclin B autophosphorylation site (*11*) and suggests a partial inhibition of CDK1-as with 1NM-PP1. Note

the similar decrease in pFOXM1 levels. (**D**) Median pFOXM1 intensities of populations gated as in Fig. 2D following treatment with ATRi-1 (2 µM), 1NM-PP1 (10 µM), and the CDK2i, NU6140 (4 µM). CDK1-as was inhibited for 30 minutes with 1NM-PP1 and then the ATR inhibitor was added for another 30 minutes.
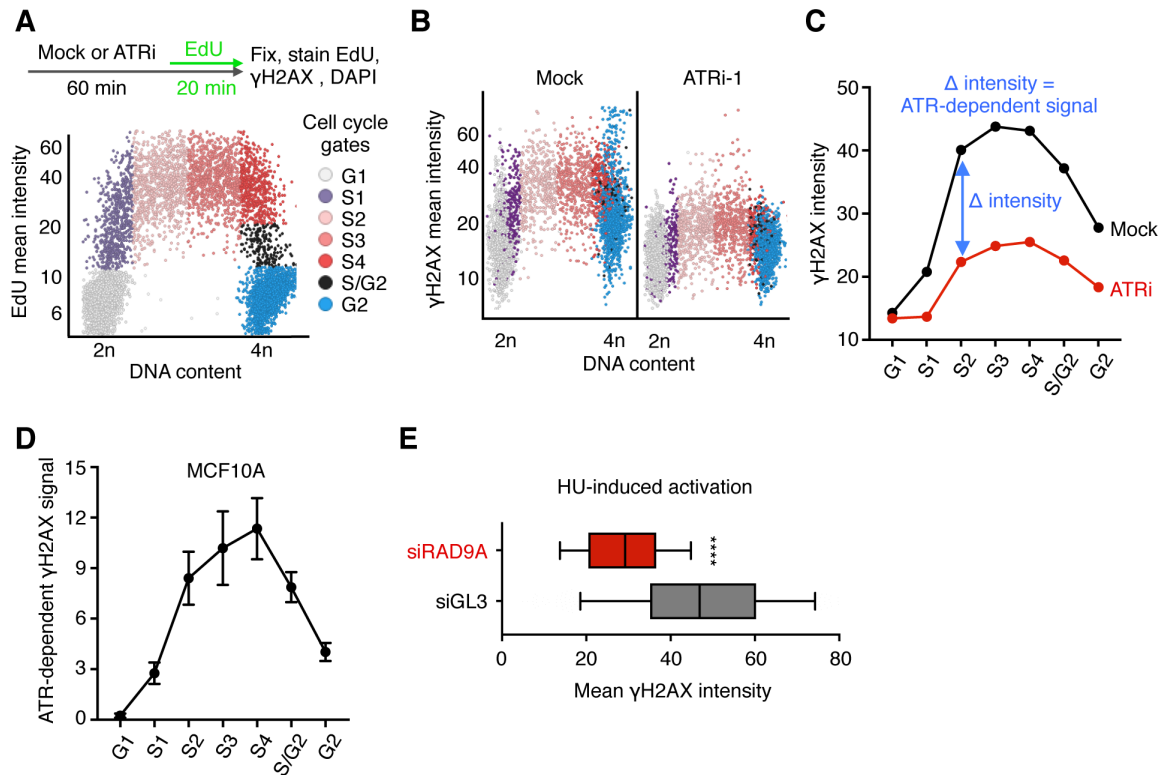
fig. S14. Analysis of ATR-dependent γH2AX signal in different cell cycle phases. (**A**) Experimental design and QIBC plots of total DAPI intensity vs EdU mean intensity. Colored dots indicate subpopulations in G1, S1-S/G2, or G2 phase. (**B**) QIBC plots of γH2AX mean intensity per nucleus versus total DAPI intensity. Colored dots indicate the subpopulations defined in (A). (**C**) Line charts from a sample experiment of the median γH2AX intensity for each subpopulation. The blue arrow indicates the difference (Δ) in the γH2AX intensity between the mock- and the ATRi-treated cells for each sub-population. This is the ATR-dependent γH2AX signal and this difference is plotted in D. (**D**) ATR activity in MCF10A cells as defined by the ATR-dependent γH2AX signal (Δ intensity) in C. Error bars represent the SEM of 3 independent experiments. (**E**) Mean γH2AX intensity of siRNA-transfected S phase cells treated with 2 mM hydroxyurea (HU) for 1 h.
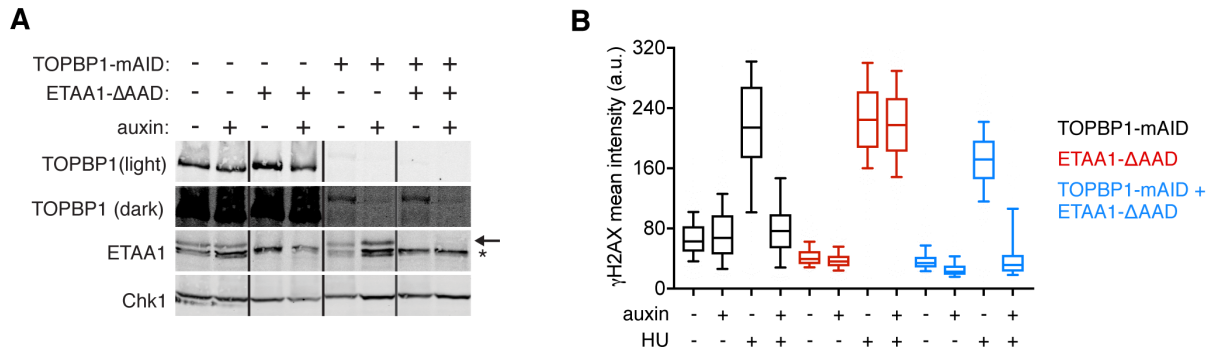
fig. S15

A

B

fig. S15. Characterization of HCT116 mutant cell lines. (**A**) Western blot analysis of TOPBP1-mAID and ETAA1 in mutant cell lines. The TOPBP1-mAID cell line expresses a TOPBP1-mAID protein that becomes rapidly degraded upon the addition of auxin. ETAA1 exon 2 was deleted in the ETAA1-ΔAAD cell line. Exon 2 encodes the ATR-activation domain (AAD). Auxin was added for 2 h. Note the ETAA1 antibody detects a non-specific band (asterisk) that migrates slightly faster than the full-length ETAA1 (arrow). Also note the decrease in TOPBP1 stability with the mAID degron without auxin. Despite this decrease in stability, these cells do not exhibit cell cycle defects or defects in genotoxin-induced ATR signaling. (**B**) γH2AX mean intensity in the HCT116 mutant cell lines treated for 2 h with auxin (0.5 mM) and/or 1 h with hydroxyurea (HU, 1 mM). Colors indicate the different HCT116 mutant cell lines.
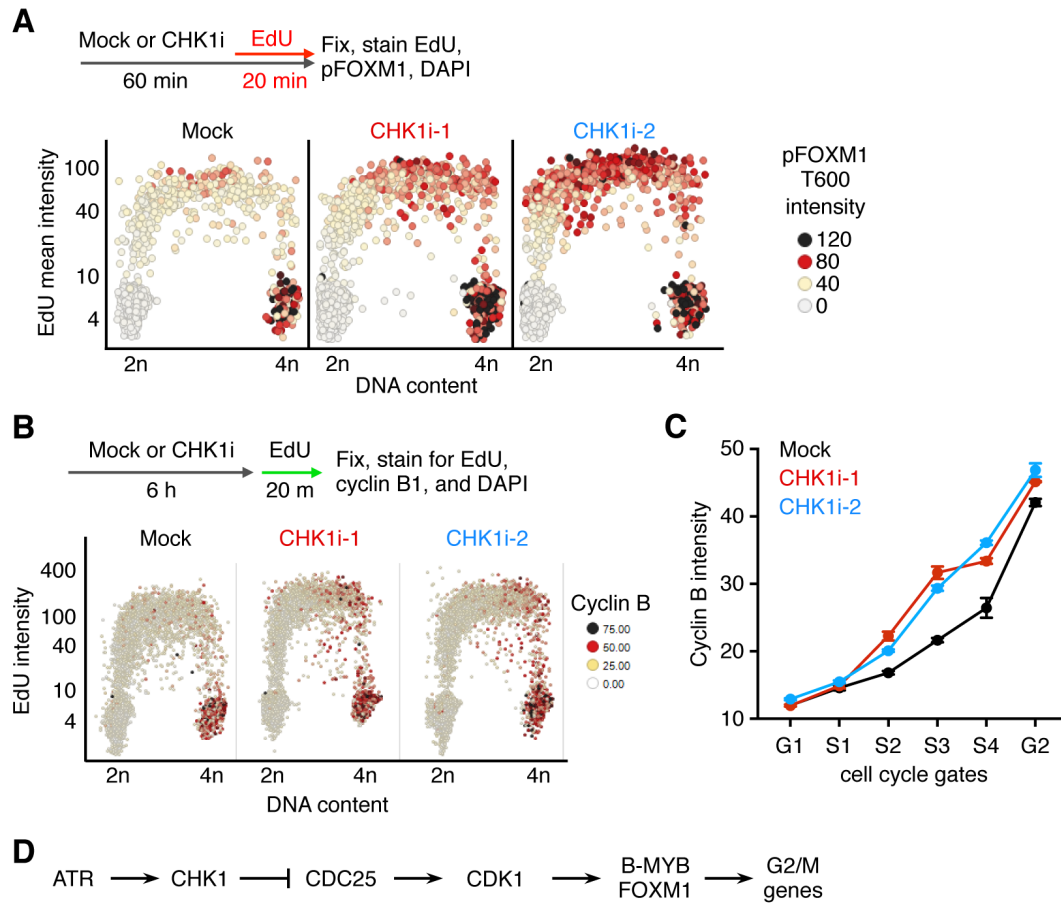
fig. S16

A

B

C

D

ATR → CHK1 ⊣ CDC25 → CDK1 → B-MYB/FOXM1 → G2/M genes

fig. S16. The ATR – CHK1 pathway suppresses the CDK-dependent hyper-phosphorylation of FOXM1. (**A**) Experimental design and QIBC plots of total DAPI intensity vs. EdU mean intensity, and mean pFOXM1 T600 intensity on a color scale. (**B**) Experimental design and QIBC plots of total DAPI intensity, EdU mean intensity, and cyclin B mean cytoplasmic intensity on a color scale. (**C**) Mean cyclin B cytoplasmic intensities of gated populations described in Fig. 1, E and F. The mitotic population was excluded. Error bars represent the SEM of cells within each gate. Cells were mock- or CHK1i-treated 2 different CHK1i for 6 h. (**D**) Schematic diagram of the signaling pathway controlling the switch-like activation of the mitotic gene network at the S/G2 transition.
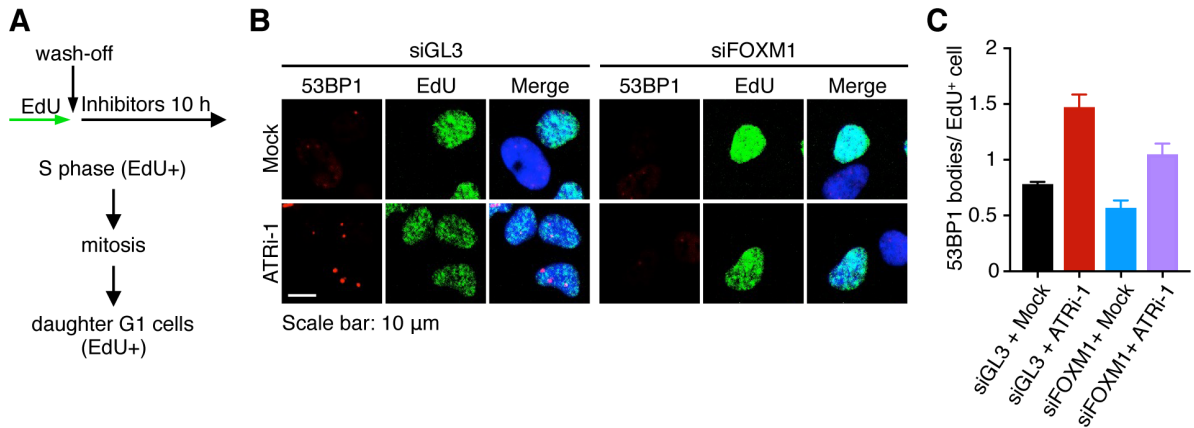
fig. S17

fig. S17. FOXM1 knockdown reduces 53BP1 body formation in ATR-inhibited cells. (**A**) Experimental design to measure 53BP1 bodies in daughter G1 cells. hTERT RPE-1 cells were transfected with siRNAs and 40 h later were pulsed with EdU (10 µM, 20 min). Following EdU wash-off, cells were mock- or ATRi-treated for 10 h. During this incubation time, the S phase cells (EdU-positive) progress though the cell cycle and divide to become the daughter G1 cells. (**B**) Representative images of 53BP1, EdU and DAPI in cells assayed as in (A). Note the presence of large 53BP1 foci (bodies) in the cells with siGL3 and ATRi-treated. (**C**) Mean 53BP1 bodies/EdU$^+$ cell in cells treated as in (A). Error bars indicated the SEM of 3 independent experiments.
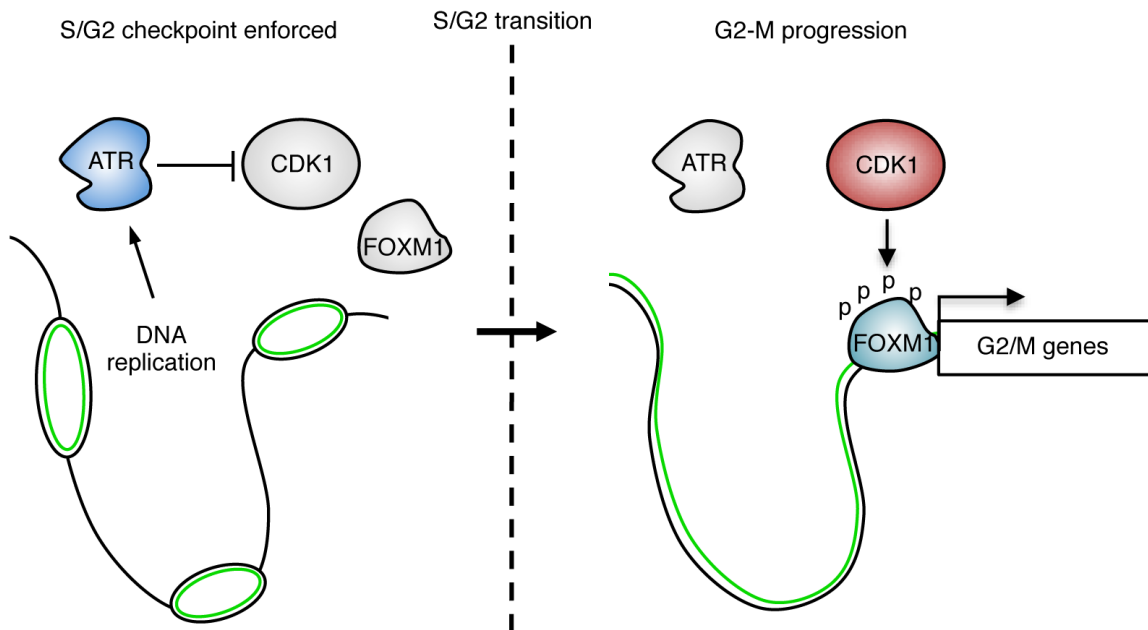
fig. S18

fig. S18. ATR enforces an intrinsic S/G2 checkpoint coordinating DNA replication and G2/M progression. ATR is activated during S phase by ongoing DNA replication. Activated ATR (blue) blocks the CDK1-dependent FOXM1 phosphorylation switch (gray). Upon the completion of DNA replication, ATR activity drops (gray) allowing CDK1 (red) to rapidly phosphorylate and activate FOXM1 at the start of G2. Once activated, FOXM1 upregulates the mitotic gene network to promote progression to mitosis. As ATR ensures G2/M progression is dependent upon the completion of S phase, we refer to this pathway as the intrinsic S/G2 checkpoint.

Table S1. List of genes in each group identified by unsupervised clustering analysis (see Fig. 1H) or shown in the volcano plot (see Fig. 1J).